

Operation-based Reliability assessment of Shore-to-Ship Fast Charging Systems

¹Siamak Karimi , ¹Mehdi Zadeh and ^{2,3}Jon Are Suul

¹Department of Marine Technology, *Norwegian University of Science and Technology (NTNU)*, Trondheim, Norway

²Department of Marine Technology, *Norwegian University of Science and Technology (NTNU)*, Trondheim, Norway

³SINTEF Energy Research, Trondheim, Norway
siamak.karimi@ntnu.no

Abstract— In this paper, the impact of charging scenario design on the reliability of for Shore-to-Ship Charging (S2SC) systems is investigated. Accordingly, the impact of the operational parameters, such as night charging planning and the onshore battery scheduling, are considered in the reliability model. To address the specific characteristics of a S2SC system, the failure threshold is calculated based on the operational parameters and system sizing. Such assessment method is conducted for a 4MW dc S2SC system. The results show that batteries and the IGBTs in dc-dc and ac-dc converters are most prone to failure. Further, it concluded that charging the onshore batteries with higher power within the allowable range can improve the reliability. Moreover, the range of onshore battery discharging power with lowest loss of charging expected is found to be between 1.5MW and 2.5MW for the studied configuration.

Keywords—marine electrification, shipboard power electronics, all-electric ship, reliability assessment, shore-to-ship charging.

I. INTRODUCTION

Shore-to-Ship Charging (S2SC) contributes to the zero-emission sea transportation by enabling the use of onboard batteries for supporting or replacing the fossil-fuel-based engines [1]. Given the availability of the sustainable energies, i.e., hydropower, solar and wind energy at the onshore grid, the battery-powered marine vessels can operate in low- or zero-emission mode, thanks to the S2SC systems [2]. Currently, 48% of all the marine vessels with onboard batteries, in operation or in order, need S2SC infrastructure. Furthermore, the dominant vessel type among these ships are the car/passenger ferries [3]. These vessels are operating in a tight schedule for commuting passengers and cars for short distances. Therefore, the onboard batteries of such vessels are recharged between the transits within a critical charging time by high power charging and over night with relatively lower charging power [2]. In these S2SC systems, any case of failure hindering the charging missions can compromise the vessel operation. In other words, a vessel which is fully or partially relying on battery charging from the onshore power system will be directly affected by any S2SC system failure. As a result, S2SC failure may lead to costly consequences and passenger dissatisfaction [4]. In this regard, the reliability of a S2SC system is defined as the probability of accomplishing the charging missions such that the vessel can operate and charge its onboard batteries according to its schedule.

System reliability estimation as part of the system configuration design routines can guarantee the performance improvement of the system. Because in such modified design routines the choice of the system elements and configurations are decided based on their impact on the estimated failure [5]. Consequently, to achieve higher reliability, the optimal redundancy, oversizing and system topology can be suggested [6], [7]. Furthermore, the reliability can be considered for the operational planning purposes. The operational planning can include the generation of the power references or the battery scheduling within the allowable range governed by the mission profile. By doing so, a system reliability improvement can be realized without adding extra components or introducing changes in the system configuration. In the literature, there are a few available studies on the mission-profile-based reliability assessment of power electronics-based systems [8], [9]. Although these methodologies are useful for operational-profile-based reliability evaluation, the impact of the operational profile within the mission profile on the reliability was not investigated. However, regarding the reliability-based operational planning, few research papers can be found in the literature [10], [11]. In [10], a reliability-based power sharing strategy for the converters in a dc microgrid is proposed. Moreover, a lifetime-based power control for converters in more electric aircrafts is introduced in [11]. The same procedure can be adapted for a S2SC system as a reliability-sensitive multi converter system with a strict mission profile.

From a reliability point of view, the critical elements in a S2SC are power electronics converters and batteries. The conventional approach for estimating the constant failure rates is MIL-HNDBK-217 [4]. Despite the fact that it has been widely used in various applications, it is not able to capture the actual operation conditions of the elements, i.e., thermal cycling and failure mechanisms [9]. On the other hand, the FIDES approach, as the most recent reliability handbook for electrical components, takes into account the physics of failure [12]. Additionally, it considers the electrical, mechanical, and thermal over stress factors to predict a real failure rate of the elements [12]. In this work, the FIDES methodology is used.

The S2SC systems usually consist of On-Shore Batteries (OSB) in addition to the Grid interface (GI) as the main sub-systems in the source side, especially in remote locations with weak onshore grid. Further, the load side is

the On-Board Batteries (OBB). Thus, the operational constraints shall meet the energy balance equations and State of Charge (SoC) limits of these batteries. Violating any of those constraints cause a failure. To address these issues, there is a need for obtaining the failure threshold of the system for specific mission profile and the system sizing. In this work, the impact of operational planning on the reliability of the S2SC system is investigated. The operational planning includes the load sharing between the onshore battery and grid within the OBB charging period for the nominal charging energy requested. It also includes the fast charging and overnight charging scheduling of both the OSB and OBB. Notably, such reliability analysis is carried out for a specific design configuration but for various scheduling scenarios. The rest of the paper is organized in the following order. First, the shore-to-ship charging systems are described introduced in terms of system configuration and operation analysis in section II. Then, the reliability methodology is illustrated through a flowchart following its step-by-step explanation in section III. Finally, the results of the reliability assessment with regard to different operational planning scenarios are presented in section IV.

II. SHORE-TO-SHIP CHARGING SYSTEMS

In this section, firstly, the system configuration of the shore-to-ship charging system under study is described. Then, the daily operational profile of such systems is illustrated through an example of a short-distanced car ferry mission profile with fast and slow S2SC.

A. System configuration

The case study considered in this paper is a battery-supported dc S2SC system for an all-electric marine vessel with the main dc bus. This system is inspired by a demonstrated project [13] and the modification suggested in [14]. The simplified single line diagram of the assumed charging system is depicted in Fig. 1. The focus of this reliability study is the onshore subsystems, the GI and OSB. The OBB sub-system is not included in this study, since the operation and maintenance of a S2SC system is often carried out by a different operator with the specific criteria compared to the onboard power system. This

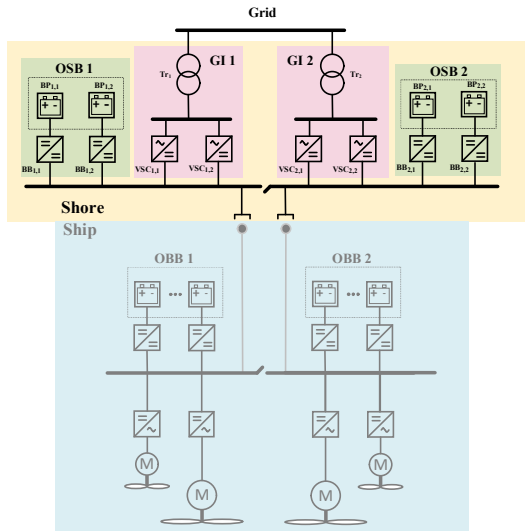


Fig. 1. The S2SC system under study.

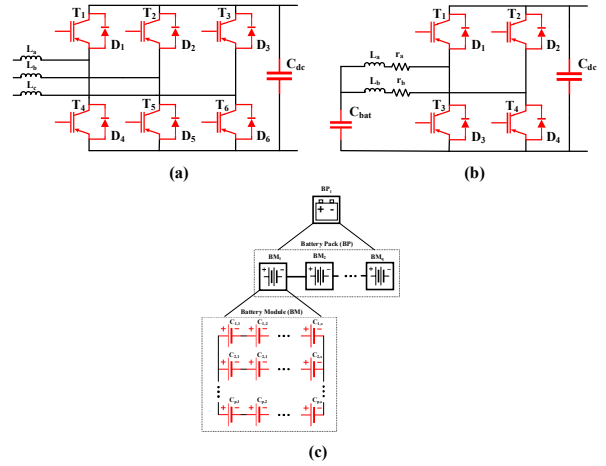


Fig. 2. The schematic of (a) the dc-ac converter ($VSC_{i,j}$), (b) the bidirectional dc-dc converter ($BB_{i,j}$), and (c) the battery pack ($BP_{i,j}$). The critical elements for reliability analysis are colored by red.

charging system is capable of supplying 4MW with installed 2MWh Li-ion onshore battery. The Voltage Source Converters ($VSC_{i,j}$) in the GI sub-system, the bidirectional interleaved Buck/Boost converters ($BB_{i,j}$) and battery packs ($BP_{i,j}$) in the OSB sub-systems are designed and depicted in Fig. 2.

B. Operation analysis

The operational profile of a S2SC system for a short-distanced ferry is usually made up of two types of recharging scenarios: 1) the opportunity charging while the vessel is loading/unloading and 2) the overnight charging with lower charging power. An example of the operational profile is shown in Fig. 3. Assuming that the energy consumption and trip time of the transit intervals and the charging power and charging time of the charging breaks are identical during one day, the operational characteristics of the case study is listed in Table I.

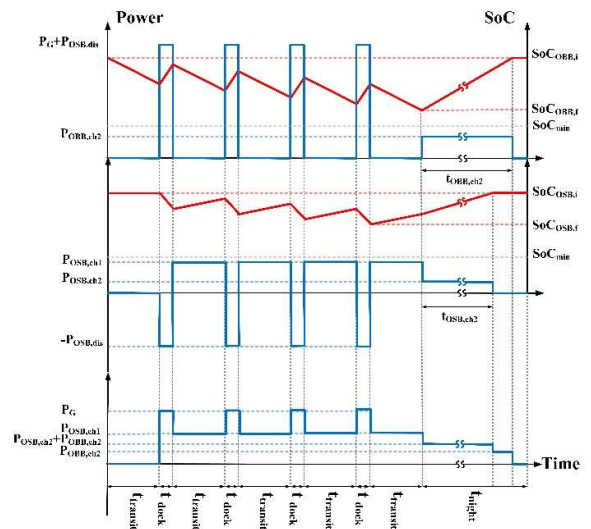


Fig. 3. An example of S2SC operational profile for a short-distanced ferry for 24 hours. a) OBB, b) OSB and GI (the blue and red profiles are the power and the SoC, respectively)

TABLE I. THE CASE STUDY CHARACTERISTICS

Parameter	Value
Number of trips per day (n)	5
Averaged docking time (t_{dock})	25 min
Averaged sailing time between charging ($t_{transit}$)	2h
Energy consumption in one trip (E_{tr})	1677kWh
Battery SoC safety range ($SoC_{Min} - SoC_{Max}$)	15%-90%

According to the operational profile in Fig. 3, the energy balance of OBB in 24 hours can be obtained as follows.

$$(n-1)[(P_{OSB,dis} + P_G)(t_{OBB,ch1})] \quad (1)$$

$$+(P_{OBB,ch2})(t_{OBB,ch2}) = nE_{tr}$$

in which $P_{OSB,dis}$, P_G and $P_{OBB,ch2}$ are the discharging power from OSB, the drawn power from grid to charge the OBB during for fast charging and overnight charging. $t_{OBB,ch1}$ and $t_{OBB,ch2}$ are the fast and slow charging times for which the following constraints shall be met within the vessel schedule:

$$0 \leq t_{OBB,ch1} \leq t_{dock} \quad (2)$$

in which t_{dock} is the docking time of the vessel. The final OBB SoC at the end of the last transit can be calculated as follows:

$$SoC_{OBB,final} = SoC_{OBB,initial} + \frac{1}{C_{OBB}}[-nE_{tr}] \quad (3)$$

$$+(n-1)[(P_{OSB,dis} + P_G)(t_{OBB,ch1})]$$

The same procedure can be done for the OSB.

$$(n-1)[(P_{OSB,dis})(t_{OBB,ch1})] \quad (4)$$

$$= (n-1)[(P_{OSB,ch1})(t_{OSB,ch1})]$$

$$+(P_{OSB,ch2})(t_{OSB,ch2})$$

$$0 \leq t_{OSB,ch1} \leq t_{transit} \quad (5)$$

$$SoC_{OSB,final} = SoC_{OSB,initial}$$

$$+ \frac{1}{C_{OSB}}[-(n-1)(P_{OSB,dis})(t_{OBB,ch1})] + \quad (6)$$

$$(n-1)(P_{OSB,ch1})(t_{OSB,ch1})]$$

in which $P_{OSB,ch1}$, $t_{OSB,ch1}$ and $P_{OSB,ch2}$, $t_{OSB,ch2}$ are the charging power and time for daytime charging and overnight charging of OSB.

III. RELIABILITY ANALYSIS

The reliability of a S2SC system is defined as the probability of recharging the onboard batteries by sufficient energy such that the vessel can operate as planned without

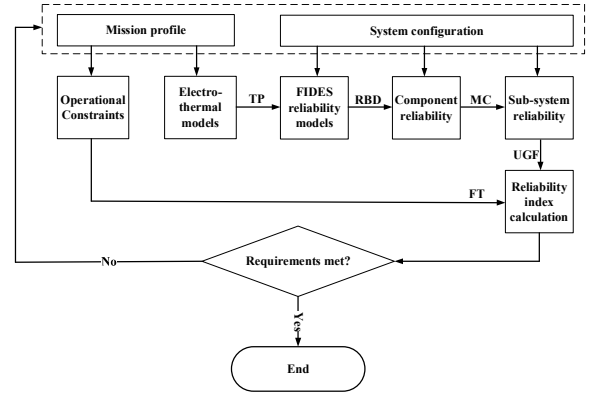


Fig. 4. The operational-profile-based reliability analysis. (TP: Temperature Profile, RBD: Reliability Block Diagram, MC: Markov Chain, FT: Failure Threshold)

any delay. The charging system consists of several reliability-critical components, such as power electronics converters and batteries. The reliability evaluation method with application-specific indices for assessing the S2SC systems are presented in [14], [4]. Here, since the variables of the reliability assessment is the operation parameters rather than the system configuration design, some modifications are to be taken into account. The flowchart illustrating the methodology is shown in Fig. 3. In the following, different stages of this flowchart will be described.

A. Operational constraints and the failure threshold

The calculation of the failure threshold for a charging system is necessary to classify the operation states into normal, derated and the final failure. Since the batteries are the load, reduced charging energy at each charging interval leads into a final state of the charge lower than the planned value. Thus, a charging system with reduced capacity may be able to charge the battery such that the vessel can operate within the minimum allowable SoC but at expense of higher overnight charging power. Further, the derated charging mission can cause that the onboard battery SoC to violate the predefined limits [4]. However, assuming 24 or 48 hours of repair time, as long as the SoC does not pass the safety SoC of the batteries, the charging can function without any induced delay on the vessel schedule. Therefore, given the operational parameters, the failure threshold can be obtained by placing $SoC_{OSB,final}$ and

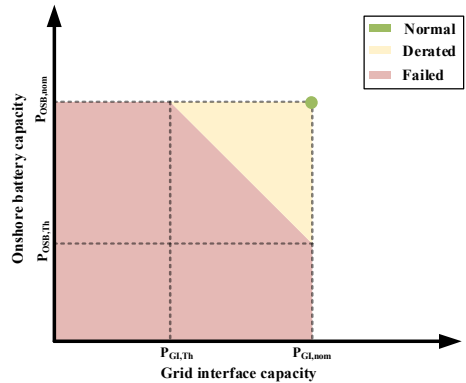


Fig. 5. The failure threshold in terms of GI and OSB capacities.

$SoC_{OBB,final}$ to be equal to SoC_{min} in (3) and (6). Further, the (1) and (4) must hold for the energy balance. Finally, regarding the availability of the system to charge the OSB between the transit intervals, the $P_{OSB,ch1}$ is chosen as following:

$$P_{OSB,ch1}^{cap} = \min(P_{OSB}^{cap}, P_{GI}^{cap}, P_{OSB,ch1}^{ref}) \quad (7)$$

By so doing, a range of capacities of GI and OSB can be calculated as depicted in Fig. 5.

B. FIDES reliability models

To estimate the constant failure during the useful lifetime for the critical parts of the S2SC system, the FIDES approach is chosen. This approach is selected due to its credibility in applying physics-of-failure-based estimation methods and considering the annual mission profile [12]. The failure rate can be calculated as follows:

$$\lambda = \Pi_{PM} \Pi_{Process} \lambda_{phy} \quad (8)$$

In which Π_{PM} is accounting for the effect of the quality and technical control over manufacturing. $\Pi_{Process}$ represents the impact of the processes from specification to field operation and maintenance. To comply with FIDES failure rate estimation, the annual mission profile must be divided into a sequence of phases. λ_{phy} is the physical contribution which is calculated in each phase regarding the thermal, mechanical and the other relevant failure mechanisms for the element. The physical contribution to the failure rate can generally be obtained as follows:

$$\lambda_{phy} = \sum_i^{phases} \left[\frac{t_{annual}}{8760} \right] \Pi_i \lambda_i \quad (9)$$

$$\Pi_i = (\Pi_{placement} \Pi_{App} \Pi_{Rugg})^{0.511 \cdot \ln(C_{sensitivity})} \quad (10)$$

$$\lambda_i = \sum_k \lambda_{0k} \Pi_k \quad (11)$$

In which t_{annual} is the duration of i^{th} phase per year. Further, Π_i is the induced electrical, mechanical and thermal overstress factors for each phase which can be calculated based on the instructions in [12]. The failure rate for each phase is called λ_i and is calculated by summing up the component-specific base failure rates, λ_{0k} , multiplied by its correspondent acceleration factors, Π_k . Such acceleration factors and base failure rates are dependent on the design aspects, case types, the temperature, humidity, and mechanical stress during each phase. Note that the dormant phases are also considered in this method.

C. The multi-layer reliability framework

From the reliability point of view, the system hierarchy is, from bottom to top, made up of 1) parts, i.e., IGBTs and capacitors, 2) components, such as, power converters and

battery packs, 3) sub-systems, GI and OSB and 4) the whole S2SC system. Thus, after calculation of the failure rates of the parts by the FIDES approach, the failure rates of the components are obtained using series reliability block diagram. Next, for each sub-system, the Markov chain of the units, a set of components connected in series, are drawn. In this stage, having the repair rates, the probability of the operation states with their capacity is calculated. Using the Universal Generating Functions, the probability characteristics of the whole system is derived. Such multi-layer reliability framework is explained in [14]. Given the failure threshold calculated based on the operation profile, the reliability indices listed in Table II can be obtained.

TABLE II. THE S2SC-SPECIFIC RELIABILITY INDICES [4].

Reliability index	Value
Loss of Charging Expected (LOCE)	$365 \sum_{i=1}^n \Pr(P_{ch} < P_{ch}^{Th})$
Derated Charging Expected (DCE)	$365 \sum_{i=1}^n \Pr(P_{ch}^{Th} < P_{ch} < P_{req-i})$
Available Charging Power (ACP)	$\sum_{i=1}^m \Pr(P_{ch,i}) \cdot P_{ch,i}$

IV. RESULTS

In this section, the case study, the system configuration, and operation described in section II are considered for the reliability assessment. In addition to the operational characteristics of the case study in Table I, the operational parameters mentioned in equations (1)-(6) are listed in Table III. For the power converters, the IGBT modules are FF1500R17IP5P [15].

TABLE III. THE OPERATIONAL PARAMETERS

Parameter	$P_{OSB,dis}$	$P_{OBB,ch1}$ $t_{OBB,ch1}$	$P_{OBB,ch2}$ $t_{OBB,ch2}$	$P_{OSB,ch1}$ $t_{OBB,ch1}$	$P_{OSB,ch2}$ $t_{OSB,ch2}$
Value	2MW	4MW 25min	400kW 196min	400kW 2h	100kW 8h

Based on the reliability assessment method depicted in Fig. 4, the reliability indices and the failure rates are calculated and listed in Table IV. Such results are compared with the calculated indices by the MIL-HNDBK-217 for the same case study in [14].

TABLE IV. THE CALCULATED RELIABILITY INDICES

Index	LOCE	DCE	ACP
FIDES-based analysis	1.46 CB/y	31.93 CB/y	3984.97 kW
MIL-HNDBK-217-based analysis [14].	2.80 CB/y	35.83 CB/y	3986.75 kW

As it is shown in Table IV, according to the FIDES-based assessment, it is expected that 1.46 and 31.93 charging breaks per year are stopped and derated, respectively. While, the MIL-HNDBK-217-based

reliability method estimates 2.8 and 35.83 charging breaks per year are stopped and derated. Thus, it can be concluded that the FIDES reliability analysis estimates the failures more optimistically, since it does not consider only the worst-case operation point to calculate the failure rates.

The calculated failure rates for the parts and components are shown in Fig. 6. Note that to calculate the failure rate of the battery packs, based on the FIDES approach, two types of the failure rates are calculated for the battery packs: 1) the cell-based constant failure rate which is estimated based on the equation (7) and 2) wear-out failure rate which is dependent on the lifetime of the battery [12].

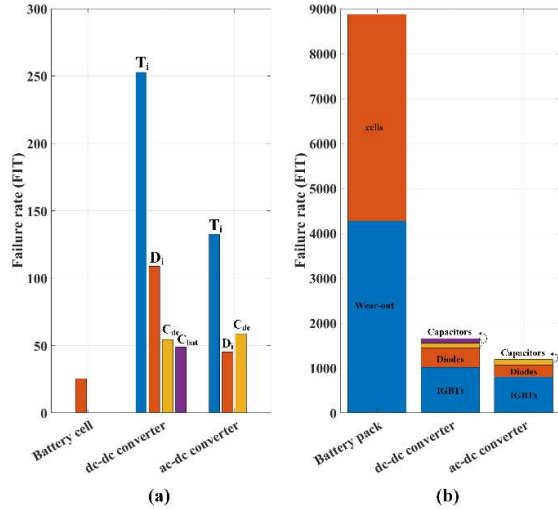


Fig. 6. The estimated failure rates based on FIDES handbook for (a) the parts and (b) the components.

It can be concluded from the, that the IGBTs and Diodes have the highest failure rates in both the power converters. Regarding the capacitor failure rates, their voltage stress factor is chosen to be less than 0.5, thereby minimizing their failure rate. Further, in the component level, the battery packs are much more prone to failure compared to the dc-dc and ac-dc converters.

In order to investigate the impact of the operational planning on the calculated reliability, feasible planning scenarios regarding the selected operational parameters are introduced. Accordingly, the trend of reliability with respect to those operational variables are interpreted.

First, the effect of the load sharing between the OSB and grid for charging OBB on the reliability indices are investigated. Notably, the OSB charging intervals between the trips are adapted to the amount of the OSB discharged energy within the docking time. In this regard, based on the capacity of the converters and the batteries, two scenarios are defined and listed in Table V. The other operational parameters are kept constant as given in Table III. The calculated reliability indices in terms of load sharing scenarios are depicted in Fig. 7.

TABLE V. THE LOAD SHARING SCENARIOS

Parameter	$P_{OBB, ch1}$	$P_{OSB, dis}$	$P_{OSB, ch1}$	$t_{OSB, ch1}$
Scenario #1	4MW	1~3MW	200~600kW	120 min
Scenario #2	4MW	1~3MW	600kW	40~120 min

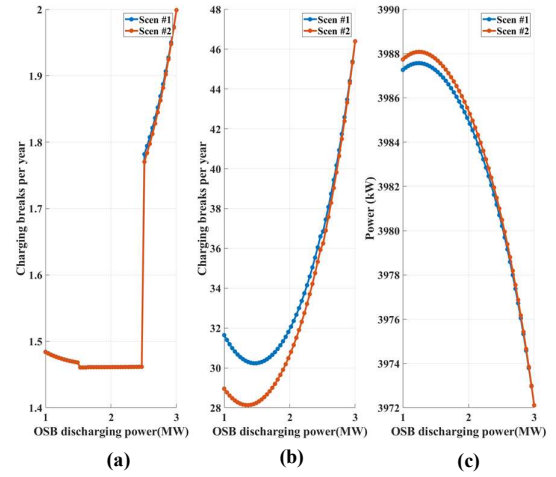


Fig. 7. The (a) LOCE, (b) DCE and (c) ACP for load sharing scenarios.

Based on the Fig. 7 (a), it can be concluded that the LOCE is quite similar for both scenarios, and for the OSB charging power between 1.5 to 2.5 MW the expected lost charging breaks are minimized for the applied range. Regarding the expected derated charging breaks, according to Fig. 7 (b), the scenario #2 with variable OSB charging time is the advantageous scenario. The lowest DCE occurs for the 1.5 MW OSB discharging power with 300 kW OSB charging power for the first scenario. Moreover, in scenario #2, the lowest DCE is for 1.4 MW OSB discharging power and 51 min OSB charging time. By looking at the calculated ACP in Fig. 7 (c), it can be seen that the second scenario for load sharing leads into the higher available charging power.

Next, the choice of the overnight charging power for both the OBB and OSB is evaluated in terms of the reliability. To this end, by keeping the operational parameters other than the night charging parameters, the reliability indices are calculated for OBB and OSB and are shown in Fig. 8 and Fig. 9.

According to Fig. 8, it can be concluded that the increase in the OBB night charging power can slightly deteriorate the reliability. Note that, the onboard battery packs are not considered in this study. As it is obvious from Fig. 9 (b), the increase of OSB night charging power by four times can decrease the DCE by 4.5 CB/yr. However, the index change per charging power steps is decreasing as the charging power increases. All in all, It can be concluded the impact of OSB night charging power is higher than that for OBB, because of the onshore battery packs with relatively large failure rates

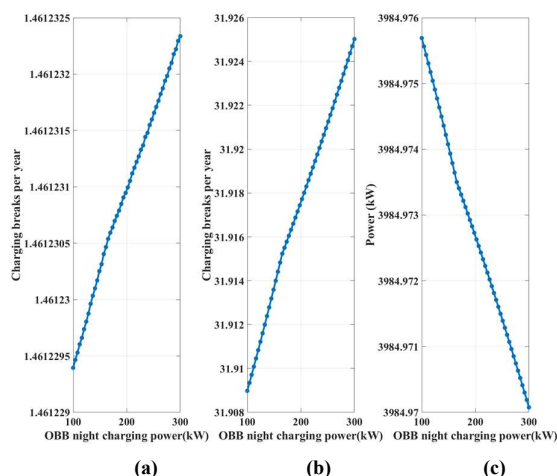


Fig. 8. The (a) LOCE, (b) DCE and (c) ACP for OBB night charging.

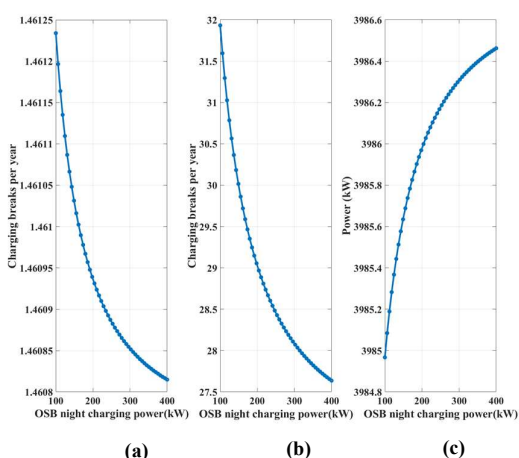


Fig. 9. The (a) LOCE, (b) DCE and (c) ACP for OSB night charging.

V. CONCLUSION

In this work, the reliability of a S2SC system is assessed using FIDES approach. This approach takes into account the mission profile and the physics-of-failure to estimate the constant failure rates. The S2SC system case study is a 4MW dc charging system with onshore batteries and grid interface sub-systems located onshore. In order to assess the S2SC as via the application-specific reliability indices, there is a need for determining a failure threshold. Such threshold, which classifies the operation into normal, derated and faulty, was calculated for a specific set of operational profile. The estimated failure rates of the IGBTs are the dominant failure rates in dc-dc and ac-dc converters. In total, the battery packs have the highest failure rates among other components.

In addition to the reliability assessment, the impact of the operational parameters on the reliability is investigated. Employing FIDES approach, the mission profile is interpreted into power references and charging/discharging scheduling. For the load sharing ratio between the onshore batteries and the grid, two scenarios were defined and tested for the reliability. The results showed that for the applied design parameters of the case study, the increase of the onshore battery discharging power can improve the reliability below 1.5 MW and deteriorate it for values larger

than 1.5MW. Further, it was concluded that the increase of the night charging power for the onshore batteries can lead into more reliable S2SC.

This reliability modeling can be employed for establishing a mixed integer nonlinear programming optimization problem to identify the operational parameters. Additionally, this model is compatible with the ship profile to realize a comprehensive reliability-oriented charging and transit profile optimization for all-electric or plug-in hybrid vessels.

REFERENCES

- [1] S. Karimi, M. Zadeh and J. A. Suul, "Shore Charging for Plug-In Battery-Powered Ships: Power System Architecture, infrastructure, and Control," *IEEE Electrification Magazine*, vol. 8, no. 3, pp. 47-61, Sept. 2020.
- [2] S. Karimi, M. Zadeh, J. A. Suul, "Evaluation of Energy Transfer Efficiency for Shore-to-Ship Fast Charging Systems," in *2020 IEEE 29th International Symposium on Industrial Electronics (ISIE)*, Delft, Netherlands, 2020.
- [3] DNV-Maritime, "Alternative Fuel Insights (AFI)," [Online]. Available: <https://afi.dnvgl.com/>. [Accessed 28 June 2021].
- [4] S. Karimi, M. Zadeh and J. A. Suul, "Reliability Analysis of Shore-to-Ship Fast Charging Systems," in *2021 IEEE Transportation Electrification Conference & Expo (ITEC)*, Chicago, US, 2021.
- [5] J. Guo, X. Wang, J. Liang, H. Pang and J. Goncalves, "Reliability Modeling and Evaluation of MMCs Under Different Redundancy Schemes," *IEEE Transactions on Power Delivery*, vol. 33, no. 5, pp. 2087-2096, Oct. 2018.
- [6] P. Tu, S. Yang and P. Wang, "Reliability- and Cost-Based Redundancy Design for Modular Multilevel Converter," *IEEE Transactions on Industrial Electronics*, vol. 66, no. 3, pp. 2333-2342, March 2019.
- [7] X. Yu and A. M. Khambadkone, "Reliability Analysis and Cost Optimization of Parallel-Inverter System," *IEEE Transactions on Industrial Electronics*, vol. 59, no. 10, pp. 3881-3889, Oct. 2012.
- [8] S. Peyghami, H. Wang, P. Davari and F. Blaabjerg, "Mission-Profile-Based System-Level Reliability Analysis in DC Microgrids," *IEEE Transactions on Industry Applications*, vol. 55, no. 5, pp. 5055-5067, Sept.-Oct. 2019.
- [9] S. Peyghami, Z. Wang and F. Blaabjerg, "A Guideline for Reliability Prediction in Power Electronic Converters," *IEEE Transactions on Power Electronics*, vol. 35, no. 10, pp. 10958-10968, Oct. 2020.
- [10] S. Peyghami, P. Davari and F. Blaabjerg, "System-Level Reliability-Oriented Power Sharing Strategy for DC Power Systems," *IEEE Transactions on Industry Applications*, vol. 55, no. 5, pp. 4865-4875, Sept.-Oct. 2019.
- [11] V. Raveendran, M. Andresen and M. Liserre, "Improving Onboard Converter Reliability for More Electric Aircraft With Lifetime-Based Control," *IEEE Transactions on Industrial Electronics*, vol. 66, no. 7, pp. 5787-5796, July 2019.
- [12] FIDES Guide 2009 Edition, "A reliability methodology for electronic," 2010.
- [13] A. Kortsari, L. Mitropoulos, T. Heinemann and H. H. Mikkelsen, "Prototype and full-scale demonstration of next-generation 100% electrically powered ferry for passengers and vehicles: Evaluation report of the E-ferry," 2020.
- [14] S. Karimi, M. Zadeh, and J. A. Suul, "A Multi-Layer Framework for Reliability Assessment of Shore-to-Ship Fast Charging System Designs," *IEEE Transactions on Transportation Electrification*, vol. (accepted for publishing), 2021.
- [15] "IGBT Modules," Infineon, [Online]. Available: <https://www.infineon.com/cms/en/product/power/igbt/igbt-modules/>. [Accessed 25 March 2021].